*International Tables for Crystallography* (2011). Vol. A1, Section 2.1.8, pp. 90–96.



and *Pcnb*, generated from that already listed by the fourfold rotation in the normalizer of $P2_12_12$.

The tetragonal supergroups (they are space groups if for their lattice parameters the equation $a = b$ holds) $P42_12$, No. 90, $P4_22_12$, No. 94, $P\bar{4}2_1m$, No. 113, and $P\bar{4}2_1c$, No. 114, all have normalizer $C(1, 1, 1/2)4/mmm$, such that the index $i_n = 2 = 2 \times 1$. There are two translationally equivalent supergroups in each case, one with origin at 0, 0, 0; 0, 0, 1/4; 0, 0, 0; and 0, 0, 1/4, respectively, the other shifted against the first one by the translation $t(1/2, 0, 0)$ or (equivalently) by $t(0, 1/2, 0)$.

The procedure just described works fine if the symmetry of the group $\mathcal{H}$ is higher than triclinic or monoclinic. The following example shows that an infinite lattice index is acceptable.

*Example 2.1.7.4.4*

Application of the normalizers to the *t*-supergroups of $\mathcal{H} = Pmm2$, No. 25.

The affine normalizer is $\mathcal{N}_{\mathcal{A}}(Pmm2) = P(1/2, 1/2, \varepsilon)4/mmm$.

The list of *t*-supergroups of *Pmm*2 starts with *Pmmm*, No. 47. The affine normalizer $\mathcal{N}_{\mathcal{A}}(Pmmm) = P(1/2, 1/2, 1/2)m\bar{3}m$; its point group $m\bar{3}m$ is a supergroup of the point group 4/*mmm* of $\mathcal{N}_{\mathcal{A}}(Pmm2)$ such that the intersection of the point groups is 4/*mmm* and $i_P = 1$. The index $i_L = \infty$, leading to a continuous sequence of supergroups with origins at $0, 0, z_0$; $0 \le z_0 < 1/2$.

The *t*-supergroup *Pmma*, No. 51, follows. $\mathcal{N}_{\mathcal{A}}(Pmma) = P(1/2, 1/2, 1/2)Pmmm$ such that $\mathcal{D} = P(1/2, 1/2, 1/2)Pmmm$ with $i_P = 2$ and $i_L = \infty$. There is a continuous set of supergroups *Pmma*. Because of the origin shift $\boldsymbol{p} = 1/4, 0, 0$ for *Pmm*2 in the subgroup table of *Pmma*, the origins of these supergroups are placed at $1/4, 0, z_0$ with $0 \le z_0 < 1/2$. Because $i_P = 2$, there is a second set of supergroups, rotated by 90° relative to the first set, such that its (unconventional) HM symbol is *Pmmb* and its origins are placed at $0, 1/4, z_0$, $0 \le z_0 < 1/2$.

The normalizer $\mathcal{N}_{\mathcal{A}} = P(1/2, 1/2, 1/2)4/mmm$ of the last orthorhombic *t*-supergroup *Pmmn*, No. 59, has the same point-group part as that of *Pmm*2 and its translation part differs only in $z = 1/2$ instead of $z = \varepsilon$. There are no transformation data for *Pmm*2 in the subgroup table of *Pmmn*, origin choice 1. There is one set of supergroups *Pmmn* with the origins at $0, 0, z_0$ for $0 \le z_0 < 1/2$.

The tetragonal minimal supergroups *P*4*mm*, No. 99, $P4_2mc$, No. 105, and $P\bar{4}m2$, No. 115, are space groups if $a = b$ holds for the lattice parameters of *Pmm*2. The affine and Euclidean normalizers of tetragonal space groups are the same.

The normalizers $C(1, 1, \varepsilon)4/mmm$ of *P*4*mm* and $P4_2mc$ differ from $\mathcal{N}_{\mathcal{A}}(Pmm2)$ only in the translation part such that $i_P = 1$ and $i_L = 2$ and the additional translations of $\mathcal{N}_{\mathcal{A}}(Pmm2)$ relative to $\mathcal{D}$ may be represented by $t(1/2, 0, 0)$. There are two supergroups each: *P*4*mm* and $P4_2mc$, with their origins at 0, 0, 0 and 1/2, 0, 0 of *Pmm*2.

Finally, the normalizer $\mathcal{N}(P\bar{4}m2) = C(1, 1, 1/2)P4/mmm$ and there are two continuous sets of supergroups $P\bar{4}m2$ with their origins at $0, 0, z_0$ and $1/2, 0, z_0$; $0 \le z_0 < 1/2$.

### 2.1.7.5. *Derivation of the remaining minimal t-supergroups*

By the procedure discussed in Section 2.1.7.4, from a supergroup $\mathcal{G} > \mathcal{H}$ other supergroups $\mathcal{G}_j > \mathcal{H}$ could be found which are isomorphic to $\mathcal{G}$ with the same index. The question arises as to whether there exist further minimal supergroups $\mathcal{G}_q > \mathcal{H}$ isomorphic to $\mathcal{G}$ and of the same index which can not be obtained by consideration of the normalizers.

Suppose $\mathcal{G}_s > \mathcal{H}$ is such a supergroup. According to the theorem of Bieberbach for space groups, isomorphism and affine equivalence result in the same classification of the space groups, *cf.* Section 8.2.2 of *IT* A. Therefore, there exists an affine mapping $\mathsf{a}_s \in \mathcal{A}$ in the group $\mathcal{A}$ of all affine mappings which transforms $\mathcal{G}$ onto the space group $\mathcal{G}_s = \mathsf{a}_s^{-1}\,\mathcal{G}\,\mathsf{a}_s$ and does not belong to $\mathcal{N}_{\mathcal{A}}(\mathcal{H})$, $\mathsf{a}_s \notin \mathcal{N}_{\mathcal{A}}(\mathcal{H})$. Let $\mathcal{H}_s = \mathsf{a}_s\,\mathcal{H}\,\mathsf{a}_s^{-1}$ be obtained from $\mathcal{H}$ by the inverse of the transformation which transforms $\mathcal{G}$ to $\mathcal{G}_s$. Then the group $\mathcal{H}_s$ is a subgroup of $\mathcal{G}$ if and only if $\mathcal{H}$ is a subgroup of $\mathcal{G}_s$. Therefore, if the space group $\mathcal{G}$ has a subgroup $\mathcal{H}_s < \mathcal{G}$ in addition to $\mathcal{H} < \mathcal{G}$, then the space group $\mathcal{H}$ has an additional supergroup $\mathcal{G}_s > \mathcal{H}$ which can be found using the transformation of $\mathcal{H}$ to $\mathcal{H}_s$. This transformation is effective only if it does not belong to the normalizer $\mathcal{N}_{\mathcal{A}}(\mathcal{G})$, otherwise it would transform the space group $\mathcal{G}$ onto itself. Therefore, only those subgroups $\mathcal{H}_s < \mathcal{G}$ have to be taken into consideration which are not conjugate to $\mathcal{H}$ under the normalizer $\mathcal{N}_{\mathcal{A}}(\mathcal{G})$.

An example of the application of this procedure is given in Section 1.7.1 and Example 1.7.3.2.2. It refers to minimal *k*-supergroups; an example for minimal *t*-subgroups is not known to the authors.

In Sections 2.1.7.4 and 2.1.7.5 only minimal *t*-supergroups are dealt with. The same considerations can be applied to minimal *k*-supergroups with corresponding results. It was not necessary to mention the minimal *k*-supergroups here, as because of the more detailed data in the tables of this volume, the simpler procedure of Sections 2.1.7.1 and 2.1.7.2 could be used to determine the minimal *k*-supergroups.

## 2.1.8. The subgroup graphs

### 2.1.8.1. *General remarks*

The group–subgroup relations between the space groups may also be described by graphs. This way is chosen in Chapters 2.4 and 2.5. Graphs for the group–subgroup relations between crystallographic point groups have been published, for example, in *Internationale Tabellen zur Bestimmung von Kristallstrukturen* (1935) and in *IT* A (2005), Figs. 10.1.3.2 and 10.1.4.3. Three kinds of graphs for subgroups of space groups have been constructed and can be found in the literature:

(1) Graphs for *t*-subgroups, such as the graphs of Ascher (1968).
(2) Graphs for *k*-subgroups, such as the graphs for cubic space groups of Neubüser & Wondratschek (1966).
(3) Mixed graphs, combining *t*- and *k*-subgroups. These are used, for example, when relations between existing or suspected crystal structures are to be displayed. Examples are the 'family trees' after Bärnighausen (1980), as shown in Chapter 1.6, now called *Bärnighausen trees*.

A complete collection of graphs of the first two kinds is presented in this volume: in Chapter 2.4 those displaying the *translationengleiche* or *t*-subgroup relations and in Chapter 2.5 those for the *klassengleiche* or *k*-subgroup relations. Neither type of graph is restricted to maximal subgroups but both contain *t*- or *k*-subgroups of higher indices, with the exception of isomorphic subgroups, *cf.* Section 2.1.8.3 below.

The group–subgroup relations are direct relations between the space groups themselves, not between their types. However, each such relation is valid for a pair of space groups, one from each of the types, and for each space group of a given type there exists a corresponding relation. In this sense, one can speak of a relation between the space-group types, keeping in mind the difference between space groups and space-group types, *cf.* Section 1.2.5.3.

The space groups in the graphs are denoted by the standard HM symbols and the space-group numbers. In each graph, each space-group type is displayed at most once. Such graphs are called *contracted graphs* here. Without this contraction, the more complex graphs would be much too large for the page size of this volume.

The symbol of a space group $\mathcal{G}$ is connected by uninterrupted straight lines with the symbols of all its maximal non-isomorphic subgroups or minimal non-isomorphic supergroups. In general, the *maximal subgroups* of $\mathcal{G}$ are drawn on a *lower level* than $\mathcal{G}$; in the same way, the *minimal supergroups* of $\mathcal{G}$ are mostly drawn on a *higher level* than $\mathcal{G}$. For exceptions see Section 2.1.8.3. Multiple lines may occur in the graphs for *t*-subgroups. They are explained in Section 2.1.8.2. No indices are attached to the lines. They can be taken from the corresponding subgroup tables of Chapter 2.3, and are also provided by the general formulae of Section 1.2.8. For the *k*-subgroup graphs, they are further specified at the end of Section 2.1.8.3.

### 2.1.8.2. *Graphs for translationengleiche subgroups*

Let $\mathcal{G}$ be a space group and $\mathcal{T}(\mathcal{G})$ the normal subgroup of all its translations. Owing to the isomorphism between the factor group $\mathcal{G}/\mathcal{T}(\mathcal{G})$ and the point group $\mathcal{P}_{\mathcal{G}}$, see Section 1.2.5.4, according to the first isomorphism theorem, Ledermann & Weir (1996), *t*-subgroup graphs are the same (up to the symbols) as the corresponding graphs between point groups. However, in this volume, the graphs are not complete but are contracted, displaying each space-group type at most once. This contraction may cause the graphs to look different from the point-group graphs and also different for different space groups of the same point group, *cf.* Example 2.1.8.2.1.

One can indicate the connections between a space group $\mathcal{G}$ and its maximal subgroups in different ways. In the contracted *t*-subgroup graphs one line is drawn for each conjugacy class of maximal subgroups of $\mathcal{G}$. Thus, a line represents the connection to an individual subgroup only if this is a normal maximal subgroup of $\mathcal{G}$, otherwise it represents the connection to more than one subgroup. The conjugacy relations are not necessarily transferable to non-maximal subgroups, *cf.* Example 2.1.8.2.2. On the other hand, multiple lines are possible, see the examples. Although it is not in general possible to reconstruct the complete graph from the contracted one, the content of information of such a graph is higher than that of a graph which is drawn with simple lines only.

The graph for the space group at its top also contains the contracted graphs for all subgroups which occur in it, see Example 2.1.8.2.3.

Owing to lack of space for the large graphs, in all graphs of *t*-subgroups the group *P*1, No. 1, and its connections have been omitted. Therefore, to obtain the full graph one has to supplement the graphs by *P*1 at the bottom and to connect *P*1 by one line to each of the symbols that have no connection downwards.

Within the same graph, symbols on the same level indicate subgroups of the same index relative to the group at the top. The distance between the levels indicates the size of the index. For a more detailed discussion, see Example 2.1.8.2.2. For the sequence and the numbers of the graphs, see the paragraph after Example 2.1.8.2.2.

*Example 2.1.8.2.1*

Compare the *t*-subgroup graphs in Figs. 2.4.4.2, 2.4.4.3 and 2.4.4.8 of *Pnna*, No. 52, *Pmna*, No. 53, and *Cmce*, No. 64, respectively. The *complete* (uncontracted) *graphs* would have the shape of the graph of the point group *mmm* with *mmm* at the top (first level), seven point groups[7] (222, *mm*2, *m*2*m*, 2*mm*, $112/m$, $12/m1$ and $2/m11$) in the second level, seven point groups (112, 121, 211, 11*m*, 1*m*1, *m*11 and $\bar{1}$) in the third level and the point group 1 at the bottom (fourth level). The group *mmm* is connected to each of the seven subgroups at the second level by one line. Each of the groups of the second level is connected with three groups of the third level by one line. All seven groups of the third level are connected by one line each with the point group 1 at the bottom.

The *contracted graph* of the point group *mmm* would have *mmm* at the top, three point-group types (222, *mm*2 and $2/m$) at the second level and three point-group types (2, *m* and $\bar{1}$) at the third level. The point group 1 at the bottom would not be displayed (no fourth level). Single lines would connect *mmm* with 222, *mm*2 with 2, $2/m$ with 2, $2/m$ with *m* and $2/m$ with $\bar{1}$; a double line would connect *mm*2 with *m*; triple lines would connect *mmm* with *mm*2, *mmm* with $2/m$ and 222 with 2.

The number of fields in a contracted *t*-subgroup graph is between the numbers of fields in the complete and in the contracted point-group graphs. The graph in Fig. 2.4.4.2 of *Pnna*, No. 52, has six space-group types at the second level and four space-group types at the third level. For the graph in Fig. 2.4.4.3 of *Pmna*, No. 53, these numbers are seven and five and for the graph in Fig. 2.4.4.8 of *Cmce*, No. 64 (formerly *Cmca*), the numbers are seven and six. However, in all these graphs the number of connections is always seven from top to the second level and three from each field of the second level downwards to the ground level, independent of the amount of contraction and of the local multiplicity of lines.

*Example 2.1.8.2.2*

Compare the *t*-subgroup graphs shown in Fig. 2.4.1.1 for $Pm\bar{3}m$, No. 221, and Fig. 2.4.1.5, $Fm\bar{3}m$, No. 225. These graphs are contracted from the point-group graph $m\bar{3}m$. There are altogether nine levels (without the lowest level of *P*1). The indices relative to the top space groups $Pm\bar{3}m$ and $Fm\bar{3}m$ are 1, 2, 3, 4, 6, 8, 12, 16 and 24, corresponding to the point-group orders 48, 24, 16, 12, 8, 6, 4, 3 and 2, respectively. The height of the levels in the graphs reflects the index; the distances between the levels are proportional to the logarithms of the indices but are slightly distorted here in order to adapt to the density of the lines.

From the top space-group symbol there are five lines to the symbols of maximal subgroups: The three symbols at the level of index 2 are those of cubic normal subgroups, the one (tetragonal) symbol at the level of index 3 represents a conjugacy class of three, the symbol $R\bar{3}m$, No. 166, at the level of index 4 represents a conjugacy class of four subgroups.

The graphs differ in the levels of the indices 12 and 24 (orthorhombic, monoclinic and triclinic subgroups) by the number of symbols (nine and seven for index 12, five and three for index 24). The number of lines between neighbouring connected levels depends only on the number and kind of symbols in the upper level.

[7] The HM symbols used here are nonconventional. They display the setting of the point group and follow the rules of *IT* A, Section 2.2.4.

However, for non-maximal subgroups the conjugacy relations may not hold. For example, in Fig. 2.4.1.1, the space group *P*222 has three normal maximal subgroups of type *P*2 and is thus connected to its symbol by a triple line, although these subgroups are conjugate subgroups of the non-minimal supergroup $Pm\bar{3}m$.

*Example 2.1.8.2.3*

The *t*-subgroup graphs in Figs. 2.4.1.1 and 2.4.1.5 contain the *t*-subgroups of the summits $Pm\bar{3}m$ and $Fm\bar{3}m$ and their relations. In addition, the *t*-subgroup graph of $Pm\bar{3}m$ includes the *t*-subgroup graphs of the cubic summits *P*432, $P\bar{4}3m$, $Pm\bar{3}$ and *P*23, those of the tetragonal summits $P4/mmm$, $P\bar{4}2m$, $P\bar{4}m2$, *P*4*mm*, *P*422, $P4/m$, $P\bar{4}$ and *P*4, those of the rhombohedral summits $R\bar{3}m$, *R*3*m*, *R*32, $R\bar{3}$ and *R*3 *etc.*, as well as the *t*-subgroup graphs of several orthorhombic and monoclinic summits. The graph of the summit $Fm\bar{3}m$ includes analogously the graphs of the cubic summits *F*432, $F\bar{4}3m$, $Fm\bar{3}$ and *F*23, of the tetragonal summits $I4/mmm$, $I\bar{4}m2$ *etc.*, also the graphs of rhombohedral summits $R\bar{3}m$ *etc.* Thus, many other graphs are included in the two basic graphs and can be extracted from them. The same holds for the other graphs displayed in Figs. 2.4.1.2 to 2.4.4.8: each of them includes the contracted graphs of all its subgroups as summits. For this reason one does not need 229 or 218 different graphs to cover all *t*-subgroup graphs of the 229 space-group types but only 37 (*P*1 can be excluded as trivial).

The preceding Example 2.1.8.2.3 suggests that one should choose the graphs in such a way that their number can be kept small. It is natural to display the 'big' graphs first and later those smaller graphs that are still missing. This procedure is behind the sequence of the *t*-subgroup graphs in this volume.

(1) The ten graphs of $Pm\bar{3}m$, No. 221, to $Ia\bar{3}d$, No. 230, form the first set of graphs in Figs. 2.4.1.1 to 2.4.1.10.
(2) There are a few cubic space groups left which do not appear in the first set. They are covered by the graphs of $P4_132$, No. 213, $P4_332$, No. 212, and $Pa\bar{3}$, No. 205. These graphs have large parts in common so that they can be united in Fig. 2.4.1.11.
(3) No cubic space group is left now, but only eight tetragonal space groups of crystal class $4/mmm$ have appeared up to now. Among them are all graphs for $4/mmm$ space groups with an *I* lattice which are contained in Figs. 2.4.1.5 to 2.4.1.8 of the *F*-centred cubic space groups. The next 12 graphs, Figs. 2.4.2.1 to 2.4.2.12, are those for the missing space groups of the crystal class $4/mmm$ with lattice symbol *P*. They start with $P4/mcc$, No. 124, and end with $P4_2/ncm$, No. 138.
(4) Four (enantiomorphic) tetragonal space-group types are left which are compiled in Fig. 2.4.2.13.
(5) The next set is formed by the four graphs in Figs. 2.4.3.1 to 2.4.3.4 of the hexagonal space groups $P6/mmm$, No. 191, to $P6_3/mmc$, No. 194. The hexagonal and trigonal enantiomorphic space groups do not appear in these graphs. They are combined in Fig. 2.4.3.5, the last one of hexagonal origin.
(6) Several orthorhombic space groups are still left. They are treated in the eight graphs in Figs. 2.4.4.1 to 2.4.4.8, from *Pmma*, No. 51, to *Cmce*, No. 64 (formerly *Cmca*).
(7) For each space group, the contracted graph of all its *t*-subgroups is provided in at least one of these 37 graphs.

For the index of a maximal *t*-subgroup, Lemma 1.2.8.2.3 is repeated: the index of a maximal non-isomorphic subgroup $\mathcal{H}$ is always 2 for oblique, rectangular and square plane groups and for triclinic, monoclinic, orthorhombic and tetragonal space groups $\mathcal{G}$. The index is 2 or 3 for hexagonal plane groups and for trigonal and hexagonal space groups $\mathcal{G}$. The index is 2, 3 or 4 for cubic space groups $\mathcal{G}$.

### 2.1.8.3. Graphs for klassengleiche subgroups

There are 29 graphs for *klassengleiche* or *k*-subgroups, one for each crystal class with the exception of the crystal classes 1, $\bar{1}$ and $\bar{6}$ with only one space-group type each: *P*1, No. 1, $P\bar{1}$, No. 2, and $P\bar{6}$, No. 174, respectively. The sequence of the graphs is determined by the sequence of the point groups in *IT* A, Table 2.1.2.1, fourth column. The graphs of $\bar{4}$, $\bar{3}$ and $6/m$ are nearly trivial, because to these crystal classes only two space-group types belong. The graphs of *mm*2 with 22, of *mmm* with 28 and of $4/mmm$ with 20 space-group types are the most complicated ones.

Isomorphic subgroups are special cases of *k*-subgroups. With the exception of both partners of the enantiomorphic space-group types, isomorphic subgroups are not displayed in the graphs. The explicit display of the isomorphic subgroups would add an infinite number of lines from each field for a space group back to this field, or at least one line (*e.g.* a circle) implicitly representing the infinite number of isomorphic subgroups, see the tables of maximal subgroups of Chapter 2.3.[8] Such a line would have to be attached to every space-group symbol. Thus, there would be no more information.

Nevertheless, connections between isomorphic space groups are included indirectly if the group–subgroup chain encloses a space group of another type. In this case, a space group $\mathcal{X}$ may be a subgroup of a space group $\mathcal{Y}$ and $\mathcal{Y}'$ a subgroup of $\mathcal{X}$, where $\mathcal{Y}$ and $\mathcal{Y}'$ belong to the same space-group type. The subgroup chain is then $\mathcal{Y} - \mathcal{X} - \mathcal{Y}'$. The two space groups $\mathcal{Y}$ and $\mathcal{Y}'$ are not identical but isomorphic. Whereas in general the label for the subgroup is positioned at a lower level than that for the original space group, for such relations the symbols for $\mathcal{X}$ and $\mathcal{Y}$ can only be drawn on the same level, connected by horizontal lines. If this happens at the top of a graph, the top level is occupied by more than one symbol (the number of symbols in the top level is the same as the number of symmorphic space-group types of the crystal class).

Horizontal lines are drawn as left or right arrows depending on the kind of relation. The arrow is always directed from the supergroup to the subgroup. If the relation is two-sided, as is always the case for enantiomorphic space-group types, then the relation is displayed by a pair of horizontal lines, one of them formed by a right and the other by a left arrow. In the graph in Fig. 2.5.1.5 for crystal class *mm*2, the connections of *Pmm*2 with *Cmm*2 and with *Amm*2 are displayed by double-headed arrows instead. Furthermore, some arrows in Fig. 2.5.1.5, crystal class *mm*2, and Fig. 2.5.1.6, *mmm*, are dashed or dotted in order to better distinguish the different lines and to increase clarity.

The different kinds of relations are demonstrated in the following examples.

*Example 2.1.8.3.1*

In the graph in Fig. 2.5.1.1, crystal class 2, a space group *P*2 may be a subgroup of index 2 of a space group *C*2 by 'Loss of

[8] One could contemplate adding one line for each series of maximal isomorphic subgroups. However, the number of series depends on the rules that define the distribution of the isomorphic subgroups into the series and is thus not constant.

centring translations'. On the other hand, subgroups of $P2$ in the block 'Enlarged unit cell', $\mathbf{a}' = 2\mathbf{a}$, $\mathbf{b}' = 2\mathbf{b}$, $C2$ (3) belong to the type $C2$, see the tables of maximal subgroups in Chapter 2.3. Therefore, both symbols are drawn at the same level and are connected by a pair of arrows pointing in opposite directions. Thus, the top level is occupied twice. In the graph in Fig. 2.5.1.2 of crystal class $m$, both the top level and the bottom level are each occupied by the symbols of two space-group types.

*Example 2.1.8.3.2*

There are four symbols at the top level of the graph in Fig. 2.5.1.4, crystal class 222. Their relations are rather complicated. Whereas one can go (by index 2) from $P222$ directly to a subgroup of type $C222$ and *vice versa*, the connection from $F222$ directly to $C222$ is one-way. One always has to pass $C222$ on the way from $F222$ to a subgroup of the types $P222$ or $I222$. Thus, the only maximal subgroup of $F222$ among these groups is $C222$. One can go directly from $P222$ to $F222$ but not to $I222$ *etc*.

Because of the horizontal connecting arrows, it is clear that there cannot be much correspondence between the level in the graphs and the subgroup index. However, in no graph is a subgroup positioned at a higher level than the supergroup.

*Example 2.1.8.3.3*

Consider the graph in Fig. 2.5.1.6 for crystal class *mmm*. To the space group *Cmmm*, No. 65, belong maximal non-isomorphic subgroups of the 11 space-group types (from left to right) *Ibam*, No. 72, *Cmcm*, No. 63, *Imma*, No. 74, *Pmmn*, No. 59, *Pbam*, No. 55, *Pban*, No. 50, *Pmma*, No. 51, *Pmna*, No. 53, *Cccm*, No. 66, *Pmmm*, No. 47, and *Immm*, No. 71. Although all of them have index 2, their symbols are positioned at very different levels of the graph.

The table for the subgroups of *Cmmm* in Chapter 2.3 lists 22 non-isomorphic $k$-subgroups of index 2, because some of the space-group types mentioned above are represented by two or four different subgroups. This multiplicity cannot be displayed by multiple lines because the density of the lines in some of the $k$-subgroup graphs does not permit this kind of presentation, *e.g.* for *mmm*. The multiplicity may be taken from the subgroup tables in Chapter 2.3, where each non-isomorphic subgroup is listed individually.

Consider the connections from *Cmmm*, No. 65, to *Pbam*, No. 55. There are among others: the direct connection of index 2, the connection of index 4 over *Ibam*, No. 72, the connection of index 8 over *Imma*, No. 74, and *Pmma*, No. 51. Thus, starting from the same space group of type *Cmmm* one arrives at different space groups of the type *Pbam* with different unit cells but all belonging to the same space-group type and thus represented by the same field of the graph.

The index of a $k$-subgroup is restricted by Lemma 1.2.8.2.3 and by additional conditions. For the following statements one has to note that enantiomorphic space groups are isomorphic.

(1) A non-isomorphic maximal $k$-subgroup of an oblique, rectangular or tetragonal plane group or of a triclinic, monoclinic, orthorhombic or tetragonal space group always has index 2.

(2) In general, a non-isomorphic maximal $k$-subgroup $\mathcal{H}$ of a trigonal space group $\mathcal{G}$ has index 3. Exceptions are the pairs $P3m1$–$P3c1$, $P31m$–$P31c$, $R3m$–$R3c$, $P\bar{3}1m$–$P\bar{3}1c$, $P\bar{3}m1$–$P\bar{3}c1$ and $R\bar{3}m$–$R\bar{3}c$ with space-group Nos. between 156 and 167. They have index 2.

(3) A non-isomorphic maximal $k$-subgroup $\mathcal{H}$ of a hexagonal space group has index 2 or 3.

(4) A non-isomorphic maximal $k$-subgroup $\mathcal{H}$ of a cubic space group $\mathcal{G}$ has either index 2 or index 4. The index is 2 if $\mathcal{G}$ has an $I$ lattice and $\mathcal{H}$ a $P$ lattice or if $\mathcal{G}$ has a $P$ lattice and $\mathcal{H}$ an $F$ lattice. The index is 4 if $\mathcal{G}$ has an $F$ lattice and $\mathcal{H}$ a $P$ lattice or if $\mathcal{G}$ has a $P$ lattice and $\mathcal{H}$ an $I$ lattice.

### *2.1.8.4. Graphs for plane groups*

There are no graphs for plane groups in this volume. The four graphs for $t$-subgroups of plane groups are apart from the symbols the same as those for the corresponding space groups: $p4mm$–$P4mm$, $p6mm$–$P6mm$, $p2mg$–$Pma2$ and $p2gg$–$Pba2$, where the graphs for the space groups are included in the $t$-subgroup graphs in Figs. 2.4.1.1, 2.4.3.1, 2.4.2.1 and 2.4.2.3, respectively.

The $k$-subgroup graphs are trivial for the plane groups $p1$, $p2$, $p4$, $p3$, $p6$ and $p6mm$ because there is only one plane group in its crystal class. The graphs for the crystal classes $4mm$ and $3m$ consist of two plane groups each: $p4mm$ and $p4gm$, $p3m1$ and $p31m$. Nevertheless, the graphs are different: the relation is one-sided for the tetragonal plane-group pair as it is in the space-group pair $P6/m$ (175)–$P6_3/m$ (176) and it is two-sided for the hexagonal plane-group pair as it is in the space-group pair $P\bar{4}$ (81)–$I\bar{4}$ (82). The graph for the three plane groups of the crystal class $m$ corresponds to the space-group graph for the crystal class 2.

Finally, the graph for the four plane groups of crystal class $2mm$ has no direct analogue among the $k$-subgroup graphs of the space groups. It can be obtained, however, from the graph in Fig. 2.5.1.3 of crystal class $2/m$ by removing the fields of $C2/c$, No. 15, and $P2_1/m$, No. 11, with all their connections to the remaining fields. The replacements are then: $C2/m$, No. 12, by $c2mm$, No. 9, $P2/m$, No. 10, by $p2mm$, No. 6, $P2/c$, No. 13, by $p2mg$, No. 7, and $P2_1/c$, No. 14, by $p2gg$, No. 8.

### *2.1.8.5. Application of the graphs*

If a subgroup is not maximal then there must be a group–subgroup chain $\mathcal{G}$–$\mathcal{H}$ of maximal subgroups with more than two members which connects $\mathcal{G}$ with $\mathcal{H}$. There are three possibilities: $\mathcal{H}$ may be a $t$-subgroup or a $k$-subgroup or a general subgroup of $\mathcal{G}$. In the first two cases, the application of the graphs is straightforward because at least one of the graphs will permit one to find the possible chains directly. If $\mathcal{H}$ is a $k$-subgroup of $\mathcal{G}$, isomorphic subgroups have to be included if necessary. If $\mathcal{H}$ is a general subgroup of $\mathcal{G}$ one has to combine $t$- and $k$-subgroup graphs.

There is, however, a severe shortcoming to using contracted graphs for the analysis of group–subgroup relations, and great care has to be taken in such investigations. All subgroups $\mathcal{H}_j$ with the same space-group type are represented by the same field of the graph, but these different non-maximal subgroups may permit different routes to a common original (super)group.

*Example 2.1.8.5.1*

An example for *translationengleiche* subgroups is provided by the group–subgroup chain $Fm\bar{3}m$ (225)–$C2/m$ (12) of index 12. The contracted graph may be drawn by the program *Subgroupgraph* from the Bilbao Crystallographic Server, http://www.cryst.ehu.es/. It is shown in Fig. 2.1.8.1; each field represents all occurring subgroups of a space-group type: $I4/mmm$, No. 139, represents three subgroups, $R\bar{3}m$, No. 166, represents four subgroups, ... and $C2/m$, No. 12, represents nine subgroups belonging to two conjugacy classes. Fig. 2.1.8.1 is part of the contracted total graph of the *translationengleiche* subgroups of the space group $Fm\bar{3}m$, which is displayed in Fig. 2.4.1.5. With *Subgroupgraph* one can also obtain the *complete graph* between $Fm\bar{3}m$ and the set of all nine subgroups of the type $C2/m$. It is too large to be reproduced here.

More instructive are the complete graphs for different single subgroups of the type $C2/m$ of $Fm\bar{3}m$. They can also be obtained with the program *Subgroupgraph* with the exception of the direction indices. In Fig. 2.1.8.2 such a 'complete' graph is displayed for one of the six subgroups of type $C2/m$ of index 12 whose monoclinic axes point in the $\langle 110\rangle$ directions of $Fm\bar{3}m$. Similarly, in Fig. 2.1.8.3 the complete graph is drawn for one of the three subgroups of $C2/m$ of index 12 whose monoclinic axes point in the $\langle 001\rangle$ directions of $Fm\bar{3}m$. It differs markedly from the contracted graph and from the first complete graph. It is easily seen that it may be very misleading to use the contracted graph or the wrong individual complete graph instead of the right individual complete graph.

In a contracted graph, no basis transformations and origin shifts can be included because they are often ambiguous. In the complete graphs the basis transformations and origin shifts should be listed if these graphs display structural information and not just group–subgroup relations. The group–subgroup relations do not depend on the coordinate systems relative to which the groups are described. On the other hand, the coordinate system is decisive for the coordinates of the atoms of the crystal structures displayed and connected in a Bärnighausen tree. Therefore, for the description of structural relations in a Bärnighausen tree knowledge of the transformations (matrix and column) is essential and great care has to be taken to list them correctly, see Chapter 1.6 and Example 2.1.8.5.4. If one wants to list the transformations in subgroup graphs, one can use the transformations which are presented in the subgroup tables.

The use of the graphs of Chapters 2.4 and 2.5 is advantageous if general subgroups, in particular those of higher indices, are sought. As stated by Hermann's theorem, Lemma 1.2.8.1.2, a Hermann group $\mathcal{M}$ always exists and it is uniquely determined for any specific group–subgroup pair $\mathcal{G} > \mathcal{H}$. If the subgroup relation is general, the group $\mathcal{M}$ divides the chain $\mathcal{G} > \mathcal{H}$ into two subchains, the chain between the *translationengleiche* space groups $\mathcal{G} > \mathcal{M}$ and that between the *klassengleiche* space groups $\mathcal{M} > \mathcal{H}$. Thus, however long and complicated the real chain may be, there is always a chain for which only two graphs are needed: a $t$-subgroup graph for the relation between $\mathcal{G}$ and $\mathcal{M}$ and a $k$-subgroup graph for the relation between $\mathcal{M}$ and $\mathcal{H}$.

For a given pair of space-group types $\mathcal{G} > \mathcal{H}$ and a given index $[i]$, however, there could exist several Hermann groups of different space-group types. The graphs of this volume are very helpful in their determination. The index $[i]$ is the product of the index $[i_P]$, which is the ratio of the crystal class orders of $\mathcal{G}$ and $\mathcal{H}$, and the index $[i_L]$ of the lattice reduction from $\mathcal{G}$ to $\mathcal{H}$, $[i] = [i_P] \cdot [i_L]$. The graphs of $t$-subgroups (Chapter 2.4) are used to find the types of subgroups $\mathcal{Z}$ of $\mathcal{G}$ with index $[i_P]$, belonging to the crystal class of $\mathcal{H}$. From the $k$-graphs (Chapter 2.5) it can be seen whether $\mathcal{Z}$ can be a supergroup of $\mathcal{H}$ with index $[i_L]$ and thus a possible Hermann group $\mathcal{M}$. The following two examples

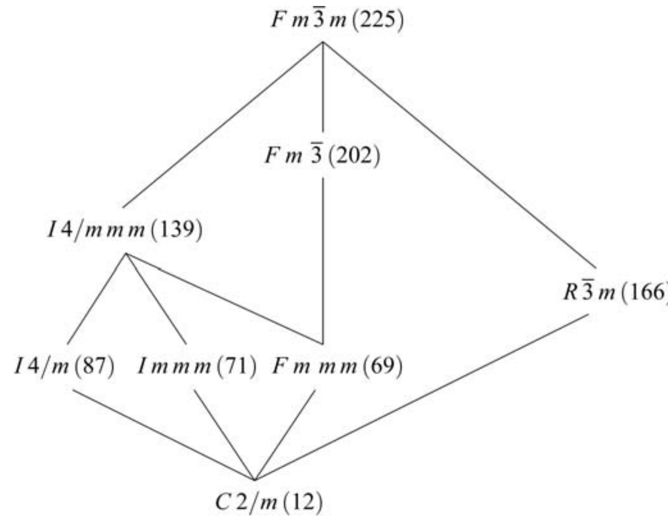


Fig. 2.1.8.1. Contracted graph of the group–subgroup chains from $Fm\bar{3}m$ (225) to one of those subgroups with index 12 which belong to the space-group type $C2/m$ (12). The graph forms part of the total contracted graph of $t$-subgroups of $Fm\bar{3}m$ (Fig. 2.4.1.5).

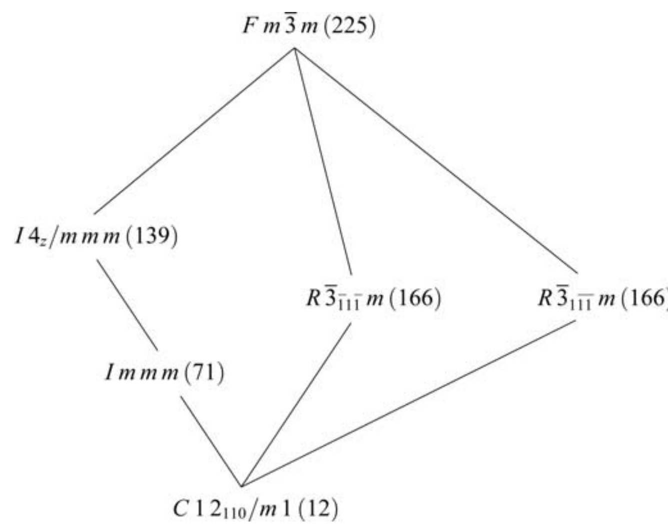


Fig. 2.1.8.2. Complete graph of the group–subgroup chains from $Fm\bar{3}m$ (225) to one representative belonging to those six $C2/m$ (12) subgroups with index 12 whose monoclinic axes are along the $\langle 110\rangle$ directions of $Fm\bar{3}m$. The direction symbols given as subscripts refer to the basis of $Fm\bar{3}m$.

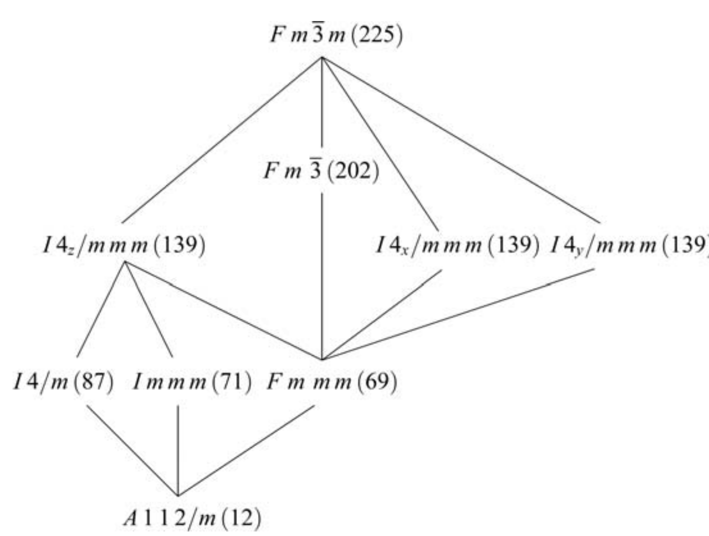


Fig. 2.1.8.3. Complete graph of the group–subgroup chains from $Fm\bar{3}m$ (225) to $A112/m$, which is one representative of those three $C2/m$ (12) subgroups with index 12 whose monoclinic axes are along the $\langle 001\rangle$ directions of $Fm\bar{3}m$.

illustrate this two-step procedure for the determination of the space-group types of Hermann groups.

*Example 2.1.8.5.2*

Consider a pair of the space-group types $Pm\bar{3}m > P2_1/m$ with index $[i] = 24$. The factorization of the index $[i]$ into $[i_P] = 12$ and $[i_L] = 2$ follows from the crystal classes of $\mathcal{G}$ and $\mathcal{H}$. From the graph of *t*-subgroups of $Pm\bar{3}m$ (Fig. 2.4.1.1) one finds that there are two space-group types, namely $P2/m$ and $C2/m$, of the relevant crystal class ($2/m$) and index $[i_P] = 12$. Checking the graph (Fig. 2.5.1.3) of the *k*-subgroups of the space groups of the crystal class $2/m$ confirms that space groups of both space-group types $P2/m$ and $C2/m$ have (maximal) $P2_1/m$ subgroups, *i.e.* space groups of both space-group types are Hermann groups for the pair $Pm\bar{3}m > P2_1/m$ of index $[i] = 24$, depending on the individual space group $P2_1/m$.

*Example 2.1.8.5.3*

The determination of the space-group types of the Hermann groups for the pair $Im\bar{3}m$ (No. 229) > $Cmcm$ (No. 63) of index $[i] = 12$ follows the same procedure as in the previous example. The index $[i] = 12$ is factorized into $[i_P] = 6$ and $[i_L] = 2$ taking into account the orders of the point groups of $\mathcal{G}$ and $\mathcal{H}$. The graph of *t*-subgroups of $Im\bar{3}m$ (Fig. 2.4.1.9) shows that the subgroups of the space-group types $Fmmm$ and $Immm$ are candidates for Hermann groups. Reference to the graph of *k*-subgroups of the crystal class $mmm$ (Fig. 2.5.1.6) indicates that $Immm$ has no maximal subgroups of $Cmcm$ type, *i.e.* only space groups of $Fmmm$ type can be Hermann groups for the pair $Im\bar{3}m > Cmcm$ of index $[i] = 12$.

Apart from the chains $\mathcal{G} \geq \mathcal{M} \geq \mathcal{H}$ that can be found by the above considerations, other chains may exist. In some relatively simple cases, the graphs of this volume may be helpful to find such chains. However, one has to take into account that the tabulated graphs are contracted ones. In particular this means that they contain nothing about the numbers of subgroups of a certain kind and on their relations, for example conjugacy relations.

The following practical example may display the situation. It is based on the combination of the graphs of Chapters 2.4 and 2.5 with the subgroup tables of Chapters 2.2 and 2.3.

*Example 2.1.8.5.4*

Let $\mathcal{G}$ be a space group of type $Pm\bar{3}m$, No. 221. What are its subgroups $\mathcal{H}_i$ of type $I4/mcm$, No. 140, and index 6?

As the order of the crystal class is reduced from cubic (48) to tetragonal (16) by index 3, the reduction of the translation subgroup must have index 2. To find the Hermann group $\mathcal{M}$, we look in the subgroup table of $Pm\bar{3}m$ for tetragonal *t*-subgroups and find one class of three conjugate maximal *t*-subgroups of crystal class $4/mmm$: $P4/mmm$, No. 123. By each of the three conjugate subgroups one of the axes **a**, **b** or **c** is distinguished. As this distinguished direction is kept in the other steps, one can take one of the conjugates as the representative and can continue with the consideration of only this representative. For the representative direction we choose the **c** axis, because this is the standard setting of $P4/mmm$. The relations of the other conjugates can then be obtained by replacing **c** by **a** or **b**.

The coordinate systems of $Pm\bar{3}m$ and $P4/mmm$ are the same, but $\mathbf{c} \neq \mathbf{a}, \mathbf{b}$ is possible for $P4/mmm$. In the subgroup table of $P4/mmm$ one looks for subgroups of type $I4/mcm$ and index 2 and finds four non-conjugate subgroups with the same basis but different origin shifts. There can be no other subgroups of type $I4/mcm$ because $P4/mmm$ is the only possible Hermann group $\mathcal{M}$. Are there other chains from $Pm\bar{3}m$ to the subgroups $I4/mcm$?

Such a new chain of subgroups must have two steps. The first one leads from $Pm\bar{3}m$ to a *k*-subgroup. In the graph for *k*-subgroups of $Pm\bar{3}m$ one finds two subgroups of index 2, namely $Fm\bar{3}m$ and $Fm\bar{3}c$. One finds from the corresponding graphs of *t*-subgroups or from the subgroup tables that only $Fm\bar{3}c$ has subgroups of space-group type $I4/mcm$. The subgroup tables of $Pm\bar{3}m$ and $Fm\bar{3}c$ show that there are two non-conjugate subgroups of type $Fm\bar{3}c$ which each have one conjugacy class of three subgroups of type $I4/mcm$. For the preferred direction **c** only one of the conjugate subgroups is relevant. Therefore, there are two subgroups $I4/mcm$ of index 2 belonging to chains passing $Fm\bar{3}c$. It follows that two of the four subgroups obtained from Hermann's group are also subgroups of $Fm\bar{3}c$ and two are not.

The two common subgroups are found by comparing their origin shifts from $Pm\bar{3}m$, which must be the same for both ways. The use of $(4 \times 4)$ matrices is convenient. The relevant equations for the bases and origin shifts are:

$$\mathbb{P}_1 = \left(\begin{array}{ccc|c} 2 & 0 & 0 & 0 \\ 0 & 2 & 0 & 0 \\ 0 & 0 & 2 & 0 \\ \hline 0 & 0 & 0 & 1 \end{array}\right) \cdot \left(\begin{array}{ccc|c} \frac{1}{2} & \frac{1}{2} & 0 & \frac{1}{4} \\ -\frac{1}{2} & \frac{1}{2} & 0 & \frac{1}{4} \\ 0 & 0 & 1 & 0 \\ \hline 0 & 0 & 0 & 1 \end{array}\right) = \left(\begin{array}{ccc|c} 1 & 1 & 0 & \frac{1}{2} \\ -1 & 1 & 0 & \frac{1}{2} \\ 0 & 0 & 2 & 0 \\ \hline 0 & 0 & 0 & 1 \end{array}\right),$$

leading to an origin shift of $(\frac{1}{2}, \frac{1}{2}, 0)$ and

$$\mathbb{P}_2 = \left(\begin{array}{ccc|c} 2 & 0 & 0 & \frac{1}{2} \\ 0 & 2 & 0 & \frac{1}{2} \\ 0 & 0 & 2 & \frac{1}{2} \\ \hline 0 & 0 & 0 & 1 \end{array}\right) \cdot \left(\begin{array}{ccc|c} \frac{1}{2} & \frac{1}{2} & 0 & \frac{1}{4} \\ -\frac{1}{2} & \frac{1}{2} & 0 & \frac{1}{4} \\ 0 & 0 & 1 & 0 \\ \hline 0 & 0 & 0 & 1 \end{array}\right) = \left(\begin{array}{ccc|c} 1 & 1 & 0 & 1 \\ -1 & 1 & 0 & 1 \\ 0 & 0 & 2 & \frac{1}{2} \\ \hline 0 & 0 & 0 & 1 \end{array}\right),$$

leading to an origin shift of $(1, 1, \frac{1}{2})$, which is equivalent to $(0, 0, \frac{1}{2})$ because an integer origin shift means only the choice of another conventional origin.

The result is Fig. 2.1.8.4, which is a complete graph, *i.e.* each field of the graph represents exactly one space group. The names of the substances belonging to the different subgroups show that the occurrence of such unexpected relations is not unrealistic. The crystal structures of $KCuF_3$ and *LT*-$SrTiO_3$ both belong to the space-group type $I4/mcm$. They can be derived by different distortions from the same ideal perovskite $ABX_3$ structure, space group $Pm\bar{3}m$ (Figs. 2.1.8.4 and 2.1.8.5). The subgroup realized by *LT*-$SrTiO_3$ is not a subgroup of $Fm\bar{3}c$. The other subgroup, which is realized by $KCuF_3$, is a subgroup of $Fm\bar{3}c$. This cannot be concluded from the contracted graphs, but can be seen from the combination of the graphs with the tables or from the complete graph (Billiet, 1981; Koch, 1984; Wondratschek & Aroyo, 2001).

The remaining two subgroups do not form symmetries of distorted perovskites. The listed orbits of the Wyckoff positions, 4*a*, 4*b*, 4*c*, 4*d* and 8*e*, are all *extraordinary orbits*, *i.e.* they have more translations than the lattice of $I4/mcm$, see Engel *et al.* (1984). In *Strukturbericht* 1 (1931) the possible space groups for the cubic perovskites are listed on p. 301; there are five possible space groups from $P23$ to $Pm\bar{3}m$. The latter space-group symbol is framed and is considered to be the *true*

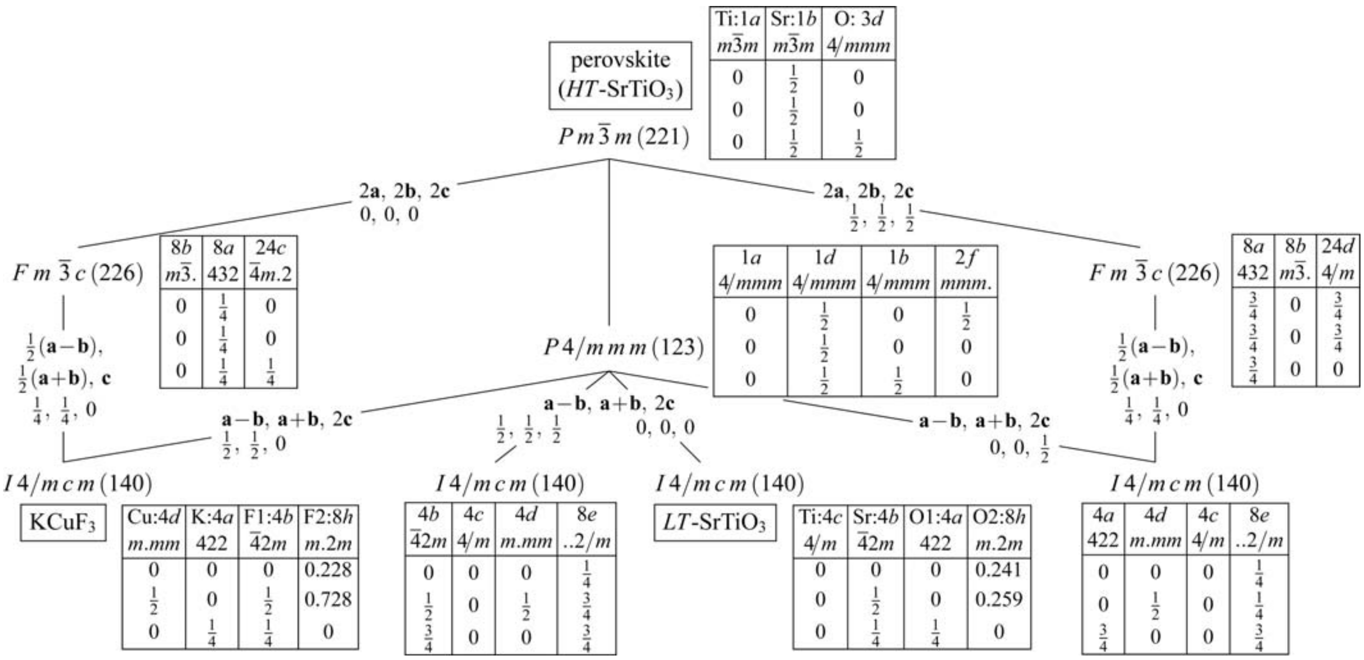


Fig. 2.1.8.4. Complete graph of the group–subgroup chains from perovskite, $Pm\overline{3}m$, here high-temperature $SrTiO_3$, to the four subgroups of type *I*4/*mcm* with their tetragonal axes in the **c** direction. Two of them correspond to $KCuF_3$ and low-temperature $SrTiO_3$. The transformations and origin shifts given in the connecting lines specify the basis vectors and origins of the maximal subgroups in terms of the bases of the preceding space groups (Bärnighausen tree as explained in Section 1.6.3).

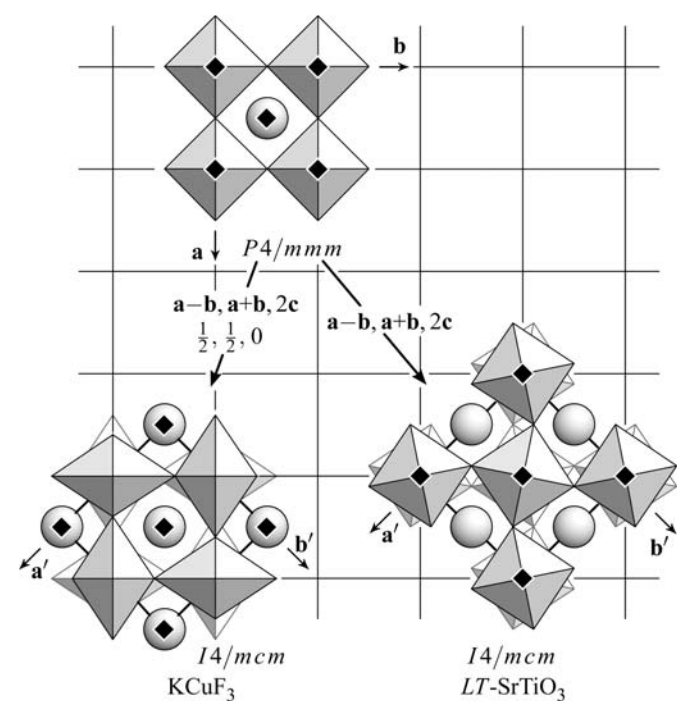


Fig. 2.1.8.5. Two different subgroups of *P*4/*mmm*, both of type *I*4/*mcm*, correspond to two kinds of distortions of the coordination octahedra of the perovskite structure. The difference is due to the origin shift by $\frac{1}{2}, \frac{1}{2}, 0$ on the left side, resulting in a different selection of the fourfold rotation axes that are retained in the subgroups.

symmetry of cubic perovskites. The other space groups are *t*-subgroups of $Pm\overline{3}m$. They would be taken if for some reason the site symmetries of the orbits would contradict the site symmetries of $Pm\overline{3}m$. Similarly, the true symmetry of these tetragonal perovskite derivatives would be *P*4/*mmm* with the original (only tetragonally distorted) lattice and not *I*4/*mcm*.[9] For the two (empty) subgroups *I*4/*mcm* a distorted variant of the perovskite structure does not exist. Other special positions or the general position of the original cubic space group have to be occupied if the space group *I*4/*mcm* shall be realized. This example shows clearly the difference between the subgroup graphs of group theory and the Bärnighausen trees of crystal chemistry.

[9] The restriction to *t*-subgroups in the space-group tables of *Strukturbericht* 1 is probably a consequence of the fact that only these subgroups of space groups were known in 1931. No tetragonal perovskites are described in that volume. In the later volumes, *Strukturbericht* 2 *ff.*, the listing of the space-group tables has been discontinued.

## References

Ascher, E. (1968). *Lattices of Equi-Translation Subgroups of the Space Groups*. Geneva: Battelle Institute.

Bärnighausen, H. (1980). *Group–subgroup relations between space groups: a useful tool in crystal chemistry. MATCH Commun. Math. Chem.* **9**, 139–175.

Billiet, Y. (1981). *Des dangers d'utiliser sans précaution des tables de sous-groupes maximum; retour au théorème d'Hermann. Acta Cryst.* A**37**, 649–652.

Engel, P., Matsumoto, T., Steinmann, G. & Wondratschek, H (1984). *The non-characteristic orbits of the space groups. Z. Kristallogr.* Supplement issue No. 1.

*International Tables for Crystallography* (2005). Vol. A, *Space-Group Symmetry*, edited by Th. Hahn, 5th ed. Heidelberg: Springer.

*International Tables for X-ray Crystallography* (1952, 1965, 1969). Vol. I, *Symmetry Groups*, edited by N. F. M. Henry & K. Lonsdale. Birmingham: Kynoch Press.

*Internationale Tabellen zur Bestimmung von Kristallstrukturen* (1935). 1. Bd. Edited by C. Hermann. Berlin: Borntraeger. (In German, English and French.)

Koch, E. (1984). *The implications of normalizers on group–subgroup relations between space groups. Acta Cryst.* A**40**, 593–600.

Ledermann, W. & Weir, A. J. (1996). *Introduction to Group Theory*, 2nd ed. Harlow: Addison Wesley Longman.

Neubüser, J. & Wondratschek, H. (1966). *Untergruppen der Raumgruppen. Krist. Tech.* **1**, 529–543.

*Strukturbericht 1913–1928* (1931). Edited by P. P. Ewald & C. Hermann. Leipzig: Akademische Verlagsgesellschaft. Continued by *Structure Reports*.

Wondratschek, H. & Aroyo, M. I. (2001). *The application of Hermann's group $\mathcal{M}$ in group–subgroup relations between space groups. Acta Cryst.* A**57**, 311–320.